Effect of Axial Ligation on the Magnetic and Electronic Properties of Lanthanide Complexes of Octadentate Ligands

Lorenzo Di Bari,[†] Guido Pintacuda,[†,‡] Piero Salvadori,[†] Rachel S. Dickins,[§] and David Parker[§]

Contribution from the Centro di Studio del CNR per le Macromolecole Stereoordinate e Otticamente Attive, Dipartimento di Chimica e Chimica Industriale, Via Risorgimento 35, I-56126, Pisa, Italy, Scuola Normale Superiore, Piazza dei Cavalieri 7, I-56126 Pisa, Italy, and Department of Chemistry, University of Durham, South Road, Durham, DH1 3LE, UK

Received April 10, 2000. Revised Manuscript Received June 28, 2000

Abstract: A detailed investigation of the solution structure of two Yb(III) complexes of C_4 symmetric chiral tetraamide ligands based on cyclen is performed in different solvents with the combined use of ^{1}H NMR, NIR-CD, and luminescence techniques. Pseudocontact chemical shifts and NOE measurements allow one to assess the relative positions of the ring and the side chains; NIR-CD spectra provide a description of the local stereochemistry around the metal ion; and finally, the axial exchange dynamics can be quantitatively characterized by means of the luminescence emission data. The two complexes can be described by a $\Lambda(\delta\delta\delta\delta)$ (i.e., square antiprismatic) coordination polyhedra, capped by a ninth axial solvent molecule. On changing the solvent composition (water, methanol, acetonitrile, dimethylsulfoxide), equilibria involving the ring or the sidearms are not detected, and the macrocycle conformation stays the same: the relevant changes in the observed spectra can thus be related to different axial coordinations. The susceptibility anisotropy factor D in the ^{1}H NMR spectra becomes progressively smaller as the strength of the axial ligand increases; correspondingly, the different crystal field caused by the varied contribution of this further ligand shapes differently the CD and the emission patterns of the central cation. The present study is the first attempt to rationalize a correspondence between the magnetic and optical parameters used in the description of the behavior of lanthanide ions in solution.

Introduction

Studies on lanthanide complexes are among the most interesting areas of contemporary chemistry: there is a steadily growing interest in the properties of these ions, which find use, for example, in organic synthesis[1]—as catalysts or reactants—and biomedicine[2,3]—as diagnostics for imaging and radiography.

The family of molecules in which the Ln^{3+} ions are caged by octadentate ligands derived from DOTA[4] has proved particularly successful: complexes with carboxylate, carboxamide, or phosphinate arms are kinetically stable over a wide pH range, and the Gd^{3+} chelates are among the most popular contrast agents for MRI.[5] Moreover, chiral analogues can constitute stereo-discriminating probes in biological media, owing to the luminescent properties of most rare-earth ions.[6]

Such complexes usually feature two stable diastereomeric structures, associated to a combination of ring and pendant arm conformations.[7] Thus, a square antiprism (with a twist angle of about 40° between the N_4 and O_4 squares) originates when the chiralities of cyclen and of the acetates layout are opposite ($\delta\delta\delta\delta$ and Λ, or $\lambda\lambda\lambda\lambda$ and Δ, respectively). It is therefore referred to as *n*-structure. On the contrary, homologous chiralities, $\Lambda(\lambda\lambda\lambda\lambda)$ or $\Delta(\delta\delta\delta\delta)$, define a *p*-diastereomer, giving rise to a distorted square antiprism (twist angle $<30°$).

In solution, interconversion between these different conformers often appears as a network of equilibria, to which a further hydration−dehydration process is superimposed.[8] This latter equilibrium has recently been shown to be dependent on the conformation of the macrocycle, with a square anti-prismatic coordination complex affording lower rates than a distorted (or twisted) anti-prismatic one.[9]

The presence of chiral substituents on the lateral chains inhibits the Λ/Δ interconversion by freezing the arm rotation;[10−12] if the center is δ to the ring nitrogen, then only one isomer is commonly observed for complexes of Eu, Tb, and Yb in solution;[13] thus, the interpretation of the properties of the

[†] Centro di Studio del CNR per le Macromolecole Stereoordinate e Otticamente Attive.

[‡] Scuola Normale Superiore.

[§] University of Durham.

(1) *Lanthanides: Chemistry and Use in Organic Synthesis*; Kobayashy, S., Ed.; Springer-Verlag: Berlin, 1999 and references therein.

(2) Evans, C. H. *Biochemistry of the Lanthanides*; Plenum Press: New York, 1990.

(3) Aime, S.; Botta, M.; Fasano, M.; Terreno, E. *Chem. Soc. Rev.* **1998**, *27*, 19−29.

(4) This and other abbreviations are: DOTA = 1,4,7,10-tetraazacyclododecane-1,4,7,10-tetraacetic acid; DOTMA = (1*R*,4*R*,7*R*,10*R*)-α,α′,α″,α‴-tetramethyl-1,4,7,10-tetraazacyclododecane-1,4,7,10-tetraacetic acid; DOTAM = 1,4,7,10-tetrakis[carbamoylmethyl]-1,4,7,10-tetraazacyclododecane.

(5) Aime, S.; Botta, M.; Fasano, M.; Terreno, E. *Acc. Chem. Res.* **1999**, *32*, 941−949.

(6) Parker, D.; Gareth Williams, J. A. G. *J. Chem. Soc., Dalton Trans.* **1996**, 3613−3628.

(7) Corey, E. J.; Bailar, J. C. *J. Am. Chem. Soc.* **1959**, *81*, 2620.

(8) Aime, S.; Botta, M.; Fasano, M.; Marques, M. P. M.; Geraldes, C. F. G. C.; Pubanz, D.; Merbach, A. *Inorg. Chem.* **1997**, *36*, 2059−2068.

(9) Aime, S.; Barge, A.; Botta, M.; De Sousa, A. S.; Parker, D. *Angew. Chem., Int. Ed.* **1998**, *37*, 2673−2674.

(10) Brittain, H. G.; Desreux, J. F. *Inorg. Chem.* **1984**, *23*, 4459−4466.

(11) Di Bari, L.; Pintacuda, G.; Salvadori, P. *Eur. J. Inorg. Chem.* **2000**, 75−82.

(12) Howard, J. A. K.; Kenwright, A. M.; Parker, D.; Port, M.; Navet, M.; Rousseau, O.; Woods, M. *Chem. Commun.* **1998**, 1381−1382.

(13) Dickins, R. S.; Howard, J. A.; Maupin, C. L.; Moloney, J. M.; Parker, D.; Riehl, J. P.; Siligardi, G.; Williams, J. A. G. *Chem. Eur. J.* **1999**, *5*, 1095−1105.

10.1021/ja0012568 CCC: $19.00
Published on Web 09/06/2000

lanthanide complex is simplified by the absence of the conformational equilibria.[14]

Chiral carboxamide ligands **1** and **2** have been extensively investigated in the past two years, and several reports have appeared on their complexes along the lanthanide series.[13,15−19] A preliminary study on the hydration properties and the axial coordination dynamics has recently been undertaken,[17−19] but no full rationalization has been put forward that accommodates all of the available experimental data.

We hereby demonstrate that for these complexes the coordination equilibrium involving a ninth axially bound ligand is independent of the ring dynamics, making it possible for the first time to assess the role of axial ligation on the main magnetic and electronic properties of the central cation (magnetic anisotropy susceptibility, crystal field parameters, absorption intensities). This is a matter of primary importance in understanding the solution behavior of such complexes: the determination of the factors governing the effectiveness of ligand exchange may, in turn, offer new insight into the design of more effective contrast agents.[5] Furthermore, since the catalytic action of lanthanide complexes is often associated with a labile coordination equilibrium involving one or more reactants in the activated state of the reaction, information about the accessibility of the rare-earth ion may be of use in modulating the catalytic activity, in rationalizing the preferred reaction pathways and in understanding the degree of stereoinduction.[1]

As a starting point for the discussion of the solution coordination properties of these complexes, the helicity of the ring and of the sidearms needs to be considered. Such an analysis begins with an examination of the solid-state data: X-ray structures of Ln-**1** complexes have been reported in the last three years, for Ln = Eu, Dy, Yb.[13,19] Although no crystal data are available for ligand **2** complexed to lanthanides, we can use as a reference the solid-state geometry of the Na^+ complex of the same ligand (*R*)-**2**.[16]

The X-ray structures reveal that Ln^{3+}−**1** and Na^+−**2** in the solid state have antiprismatic and distorted antiprismatic coordination (*n*- and *p*-forms) respectively, with the same layout of the acetate arms, leading to a Λ coordination, and the conformation of the macrocycles being $\delta\delta\delta\delta$ for Ln^{3+}−**1** and $\lambda\lambda\lambda\lambda$ for Na^+−**2**.

Structural assignment in solution by the analysis of the pseudocontact ^{1}H NMR shifts needs special care, because of the following reasons:

1. It has been reported that *n*- and *p*-forms can lead to practically equal geometrical factors.[11]

2. All of the protons which exhibit distinct pseudocontact shifts lie within an inner sphere (i.e., in the DOTA-portion of the molecule). As a consequence, no direct relation can be found to the chirotopic elements of known configuration (i.e., the amine carbons), and one cannot discern between pairs Λ($\delta\delta\delta\delta$) and Δ($\lambda\lambda\lambda\lambda$) for the antiprismatic coordination or Λ($\lambda\lambda\lambda\lambda$) and Δ($\delta\delta\delta\delta$) for the distorted antiprism.

Scheme 1

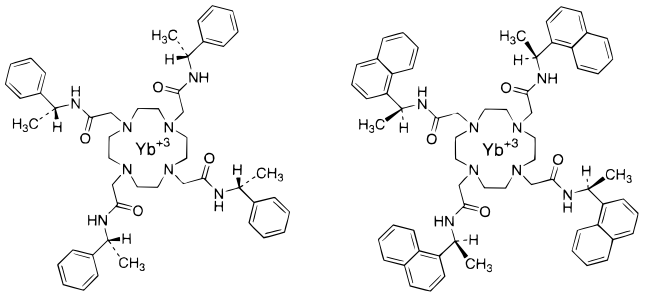

It is therefore of prime importance first, in the case of Yb−(*R*)-**1**, to confirm the persistence in solution of the conformation observed in the crystal phase and second, in the case of Yb−(*S*)-**2**, to verify whether the Na^+ solid-state complex is a good description of the geometry in solution (Scheme 1).

Once detailed information on the two coordination polyhedra is available, then a safe analysis of the magnetic and chiroptical properties of these species is made possible. While carrying out this purely structural investigation, involving the combined use of NMR and electronic spectroscopy, we became aware of the key role of axial ligation on the magnetic and electronic properties of ytterbium. A variation in the NMR spectral features of lanthanide complexes following different axial bindings has been recently detected.[20−22] This was attributed to a change in the magnetic susceptibility anisotropy, following the modification (or the expansion) of the coordination sphere. Unfortunately, it is difficult to exclude in general a simultaneous readjustment of the ligand structure.[20,22] In the only reported example involving a rather rigid macrocycle, changes in the effective crystal field parameters accompany the exchange of the anionic counterions.[21] We here take into account coordination with neutral solvent molecules. Such a process is likely to be almost ubiquitous in the solution chemistry of lanthanides, which are characterized by a large and variable coordination number. We then present a general rationalization of a number of phenomena that may be observed by studying these complexes in different solvents.

Experimental Section

Cationic enantiopure Yb−(*R*)-**1** and Yb−(*S*)-**2** complexes were obtained as their trifluoromethanesulfonate salts as previously described.[13,15,16] Solutions for ^{1}H NMR and NIR-CD spectroscopy were prepared by dissolving the solid complexes in MeOD-d_4, DMSO-d_6, and acetonitrile-d_3 or the corresponding non-deuterated solvents in the range 20−100 mM.

Chemical shifts were referenced with respect to *tert*-butyl alcohol as internal standard. ^{1}H NMR spectra were recorded on a modified Varian VXR operating at 65.3 MHz and a Varian VXR 300 spectrometer operating at 300 MHz, equipped with a VT unit stable within 0.1 °C. The 90° pulse length was 14 μs. The recycle delay in all experiments was above 0.5 s, largely exceeding $5 \cdot T_1$ of all the proton resonances investigated and ensuring instrumental recovery. Steady-state NOE spectra were recorded with up to 32768 transients after 0.5 s cw-presaturation of the relevant signals.

NIR absorbance spectra were recorded on a Perkin-Elmer Lambda 19 spectrometer, with 1 cm cells and a band-passing width of 2.5 nm.

(14) Di Bari, L.; Pintacuda, G.; Salvadori, P. *J. Am. Chem. Soc.* **2000**, *122*, 5557−5562.

(15) Dickins, R. S.; Howard, J. A. K.; Lehmann, C. W.; Moloney, J.; Parker, D.; Peacock, R. D. *Angew. Chem., Int. Ed. Engl.* **1997**, *36*, 521−523.

(16) Dickins, R. S.; Howard, J. A. K.; Moloney, J.; Parker, D.; Peacock, R. D.; Siligardi, G. *Chem. Commun.* **1997**, 1747−1748.

(17) Maupin, C. L.; Parker, D.; Williams, J. A. G.; Riehl, J. P., *J. Am. Chem. Soc.* **1998**, *120*, 10563−10564.

(18) Aime, S.; Barge, A.; Bruce, J. I.; Botta, M.; Howard, J. A. K.; Moloney, J. M.; Parker, D.; de Sousa, A. S.; Woods, M. *J. Am. Chem. Soc.* **1999**, *121*, 5762−5771.

(19) Batsanov, A. S.; Beeby, A.; Bruce, J. I.; Howard, J. A. K.; Kenwright, A. M.; Parker, D. *Chem. Commun.* **1999**, 1011−1012.

(20) Benetollo, F.; Polo, A.; Bombieri, G.; Fonda, K. K.; Vallarino, L. M. *Polyhedron* **1990**, *9*, 1411.

(21) Lisowski, J.; Sessler, J. L.; Lynch, V.; Mody, T. D. *J. Am. Chem. Soc.* **1995**, *117*, 2273−2285.

(22) Lisowski, J. *Magn. Reson. Chem.* **1999**, *37*, 287−294.

Table 1. Experimental Lanthanide-Induced Shifts (δ, in ppm) of the Yb−(*R*)-1 Amide Complex in d_4-MeOD, d_3-MeCN, and d_6-DMSO Solutions ($T = 25$ °C) and Differences $\delta_{pc}^{exp} - \delta_{pc}^{calc}$ between the Experimental Pseudocontact Contributions and Those Calculated in the Fitting Algorithm[a]

	$3\cos^2\vartheta - 1/r^3 \times 100$ (Å^{-3})		δ^{exp}			$\delta_{pc}^{exp} - \delta_{pc}^{calc}$ (*n*−form)			$\delta_{pc}^{exp} - \delta_{pc}^{calc}$ (*p*−form)		
	n-form	*p*-form	MeOH	DMSO	MeCN	MeOH	DMSO	MeCN	MeOH	DMSO	MeCN
A1	3.02	2.97	100.0	64.0	124.1	1.5	1.7	0.7	1.5	1.5	0.6
A2	−0.96	−0.97	−30.7	−17.8	−41.4	−1.4	0.04	−4.1	−1.4	0.09	−4.1
E1	0.52	0.49	16.9	11.6	19.1	−1.3	−0.4	−3.4	−1.3	−0.4	−3.4
E2	0.67	0.64	19.9	13.5	23.3	−3.3	−1.6	−5.4	−3.3	−1.6	−5.6
C1	−0.88[b]	−0.96[b]	−24.6	−13.8	−34.2	1.9	2.3	−0.5	1.7	2.3	−0.9
C2	−2.17[b]	−1.74[b]	−61.9	−35.5	−80.9	0.1	0.5	−0.3	0.2	0.4	−0.4
ω						27 ± 3	23 ± 4	34 ± 3	51 ± 3	47 ± 3	53 ± 4
$\langle r \rangle$						1.6	1.1	2.4	1.6	1.0	2.5
R, %						3.41	3.63	4.77	3.39	3.47	4.87
D						3370 ± 70	2090 ± 50	4200 ± 120	3370 ± 70	2080 ± 60	4200 ± 120

[a] The proton labeling is analogous to that commonly used for similar complexes (see ref 25). The factors on the second and third columns are calculated from the crystal structures of Yb−(*R*)-**1** as described in the text and refer to structures which are representative of a *n*- type and a *p*-type, respectively. The experimental pseudocontact shifts used in the computations are the values relative to diamagnetic free ligands. Shifts in water are not reported, but they are analogue to those reported in the table for methanol. For each set of chemical shift fitted, the dihedral angle ω of the side chain, the agreement factor $R = \sqrt{\sum_i(\delta_i^{exp} - \delta_i^{exp})^2/\sum_i(\delta_i^{exp})^2}$ and the susceptibility factor *D* are displayed. [b] These values are relative to the geometry with $\omega = 0$.

NIR-CD spectra were recorded on an upgraded JASCO J-200D dichrograph, operating between 750 and 1350 nm, modified with a tandem Si/InGaAs detector with dual photomultiplier amplifier.[23] The path length was 1 cm, and the band-passing width was 2.5 nm.

Luminescence emission spectra and radiative rate constants characterizing the decay of emission from the Yb excited state were measured using apparatus described previously.[24]

Results and Discussion

1. NMR Structural Determination. a. ^{1}H NMR Spectra. The ^{1}H NMR spectra of Yb−(*R*)-**1** and Yb−(*S*)-**2** in CD_3OD solution were measured, and the assignment of the resonances was made from the relative peak areas and by comparison with the spectral data previously reported for YbDOTA.[25] Only the protons lying close to the Yb ion (distance from Yb^{3+} $r < 5$ Å) are significantly paramagnetically shifted; they practically correspond to the DOTA-portion of the molecule, which is not involved in any observable dynamics over a wide temperature range (−40 to +40 °C). The values of the chemical shift for each assigned signal are summarized in Table 1 for Yb−(*R*)-**1**; the values for Yb−(*S*)-**2** are analogous**.** The proton shift in a lanthanide complex can be written as:

$$\delta = \delta_{dia} + \delta_{con} + \delta_{pc}$$

where the three contributions are the diamagnetic, paramagnetic contact, and paramagnetic pseudocontact terms. In the case of Yb(III), the contact contribution is usually negligible, and in the case of axially symmetric complex, the pseudocontact shift can be expressed as:

$$\delta_{pc} = D\,\frac{3\cos^2\vartheta - 1}{r^3} + \Delta \qquad (1)$$

where ϑ and *r* are the polar coordinates of a nucleus respect to the Yb(III) ion, *D* is the magnetic anisotropy factor, in units of ppm·Å^3, and a constant Δ has been introduced to take into account the bulk paramagnetism.[26]

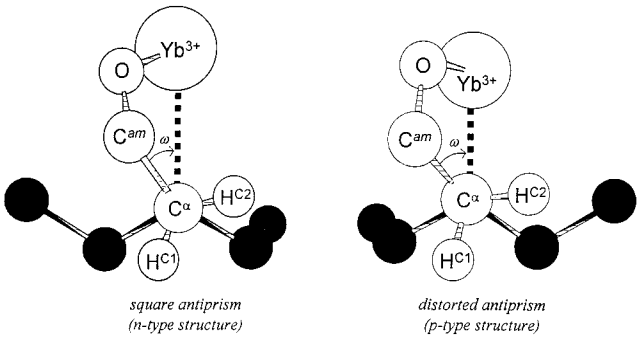

Figure 1. Position of the ring and of the side chains in the two different coordination types used as models for the fitting procedures. The pictures refer to a Newmann projection onto the N−C$^\alpha$ bond; the dihedral angle ω Yb−N−C$^\alpha$−C is also displayed. In black are depicted the carbon atoms of the cyclen macrocycle.

A set of reference geometrical factors is usually calculated from crystal structures. The X-ray structure of Yb−(*R*)-**1** provides the geometrical parameters corresponding to a square antiprism (*n*-type structure).[19] At the moment, no crystal data are available for Yb(III) complexed in a distorted square antiprism (*p*-type geometry) as found in solution for YbDOTA (minor form) or YbDOTMA (major form). Two equivalent sets of polar coordinates ϑ and *r*, with reference to eq 1, can be obtained:

1. from the solid-state geometry of Na−(*R*)-**2**;[16]

2. by manipulating the atomic coordinates of GdDOTA, with the aid of commercially available software for molecular graphics, by suitable stereochemical operations (e.g., rotation around the N−C$^\alpha$ bond, epimerization of the stereogenic center at C$^\delta$, mirror imaging), as described for YbDOTMA.[11]

The two sets of geometrical parameters obtained in this way and used for the optimization are also reported in Table 1.

It should be recalled that because the protons on the pendant arms exhibit small pseudocontact shifts, they were not used in structure calculation.

The main degree of freedom for the DOTA-portion of the molecule is the torsion angle ω around N and C$^\alpha$ (defined here as the dihedral Yb−N−C$^\alpha$−C$^\beta$ shown in Figure 1). Thus, a simultaneous fitting of ω and *D* was performed, starting from the two geometries for the *p*- and *n*-forms, as summarized in Table 1.

(23) Castiglioni, E. Book of Abstracts, 6th International Conference on CD, Pisa, September 1997.

(24) Beeby, A.; Clarkson, I. M.; Dickins, R. S.; Faulkner, S.; Parker, D.; Royle, L.; de Sousa, A. S.; Williams, J. A. G.; Woods, M. *J. Chem. Soc., Perkin Trans., 2* **1999**, 493−503.

(25) Desreux, J. F. *Inorg. Chem.* **1980**, *19*, 1319−1324.

(26) Such a constant will compensate possible effects due to paramagnetic contributions to the chemical shift of the internal reference.

From inspection of Table 1, it is apparent that no definite structural assignment for these molecules can follow from analysis of the pseudocontact contribution only. The fact that both the *n*- and *p*-type geometries lead to very similar geometrical factors shows that no clear-cut information can be obtained from 1D ^{1}H NMR spectrum as far as the conformation of the macrocycle is concerned. Such a conclusion has been noted in analyzing the two forms of YbDOTMA.[11] Moreover, while the spectra are almost the same for the two complexes, the proportionality of the two sets of geometrical factors does not exclude the possibility that Yb−(*R*)-**1** and Yb−(*S*)-**2** adopt two diastereomeric structures. Indeed, the agreement factors are almost the same for both diastereomers in each solvent.

Potentially useful information could be contained in the chemical shift of CH, methyl, and aromatic protons, which are somewhat different in the two complexes. However, this information is lost because of the local dynamics affecting this portion of the molecule, and again no safe conclusion can be drawn from the averaged values observed.

The data in Table 1 show that minor structural adjustements must occur between crystal and solution geometry, whichever of the two structural types is correct. The data suggest a counterclockwise rotation of about 10° of the acetate arm with respect to the solid-state structure for $\Lambda(\delta\delta\delta\delta)$, and the inversion of the macrocycle for $\Lambda(\lambda\lambda\lambda\lambda)$ (or their mirror images).

An empirical correlation between the ^{1}H NMR spectral width of the Yb complex, that is the value of the magnetic anisotropy factor, D, and the preferred conformation has been proposed.[19,27] With reference to the major and minor forms of YbDOTA,[25,8] it has been assumed that a value of $D \approx 5000$ in water or in methanol solution may be associated with a *n*-type structure of the ytterbium complex, while a $D \approx 3500$ is a evidence for the *p*-type molecule. Unfortunately, the *reference* molecule binds the lanthanide ions with different donor atoms: a comparison between the coordination properties of a carboxylate oxygen and an amide oxygen is neither straightforward nor safe. Moreover, such complexes are involved in different hydration−dehydration equilibria;[8] thus, the magnitude of the magnetic anisotropy is likely to be largely determined (beside the specific contribution of the octadentate cage) by the presence or absence of an axial substituent. According to Bleaney's model,[28] D is directly dependent on the crystal field experienced by the lanthanide ion, which is in turn strongly affected by a ninth capping ligand.[21,22,29]

The observation of a certain regularity in the anisotropy factor, D, is demonstrated by recording spectra of each complex in DMSO. Such a solvent has a large effect on the value of D: the spectra of both complexes, spanning about 170 ppm in MeOD, water or acetonitrile, reduce to 100 ppm in DMSO solution, with axial A_1 and acetate C_2 protons resonating at about 70 ppm and −35 ppm, respectively. Despite this difference, the pseudocontact shifts in DMSO are perfectly proportional to the corresponding values in CD_3OD and can be fitted smoothly to the two sets of geometrical factors derived from the *n*- and *p*-type structures (see Table 1). This proves that the complex possesses the same coordination, but again it is impossible to rule out either of the two possibilities for the helicity of the ring.

The observed variation of ^{1}H NMR spectral width must be connected to some variation in the properties of the central Yb cation. Furthermore, whether the conformation of the macrocycle has switched between λ/δ as a consequence of the solvent variation must be determined, as well.

Table 2. Mean Interproton Distances (Å) Obtained from the Crystal Structures of Yb−(*R*)-1 (Square Antiprism, *n*-Type Structure) and Na−(*R*)-2 (Distorted Square Antiprism, *p*-Type Structure)[a]

square antiprism (*n*-form)			distorted antiprism (*p*-form)		
proton	C_1	C_2	proton	C_1	C_2
A_1	3.31	3.88	A_1	3.54	3.37
E_2	**2.24**	3.34	E_2	2.66	2.51
A_2	2.88	**2.13**	A_2	2.39	**2.09**
E_1	2.72	2.91	E_1	2.47	3.46

[a] The values which allow the detection of a steady-state NOE are typed in boldface.

b. NOE Effects. Unequivocal evidence for the *p* or *n* conformation of the complex must be found from an independent measurement. As recently proposed in the case of YbDOTMA, information can be obtained by observing the steady-state NOE spectra following saturation of relevant ring or acetate protons. In this way, it is possible to estimate some pairwise proton distances and constrain the geometry of the complex to one of the two diastereomers.

With these complexes, this experiment is not straightforward, owing to:

- the large self-relaxation rates ρ induced by the coupling to the unpaired electron, which sizeably reduce the Overhauser enhancement η;
- the dependence of σ on the correlation time in magnitude and sign

$$\sigma \propto \frac{2}{3}J^2 - \frac{1}{3}J^0 = \frac{2\tau_c}{1-4\omega^2\tau_c^2} - \frac{\tau_c}{3}$$

At 300 MHz, such a contribution is expected to vanish for $\tau_c \approx$ 260 ps, for which no NOE can be observed.[30,31]

On saturating the C_2 resonance, a clear NOE can be obtained on the A_2 proton; furthermore, on saturating the C_1 peak, a NOE is obtained on E_2. The latter effect cannot be justified for a twisted antiprism (*p*-type structure), highlighted by the interproton distances reported in Table 2.[32] The $\Lambda(\delta\delta\delta\delta)/\Delta(\lambda\lambda\lambda\lambda)$ form can be assigned to the Yb−(*R*)-**1** complex in solution, consistent with that observed the crystal structure and different to the previous suggestion[13,19] based only on the magnitude of the anisotropy D.

The case of Yb−(*S*)-**2** is more intriguing. On saturating each of the ring protons, no NOE effect can be clearly observed on the acetate peaks nor even between geminal protons: this demonstrates that the correlation time of this complex is in the intermediate-motion region where $\sigma = 0$. To get over the problem, an ROE effect, for which the zero value never occurs, can be sought instead. It is, anyway, very difficult to effectively spin lock widely separated signals such as those under examination.[30]

It was found more convenient to act on the correlation time of the molecule, making it longer, by changing the solvent from

(27) Aime, S.; Botta, M.; Parker, D.; Williams, J. A. G. *J. Chem. Soc., Dalton Trans.* **1995**, 2259−2266.
(28) Bleaney, B. *J. Magn. Reson.* **1972**, *8*, 91−100.
(29) Hüfner, S. *Optical spectra of transparent Rare Earth Compounds*; Academic Press: New York, 1978.
(30) Bertini, I.; Luchinat, C. *Coord. Chem. Rev.* **1996**, *150*, 1−296.
(31) Ernst, R. R.; Bodenhausen, G.; Wokaun, A. *Principles of NMR in one and two dimensions*; Clarendon Press: Oxford, 1987.
(32) From the signal-to-noise ratio of the Overhauser effect between the two geminal acetate protons after 32 K acquisitions, the limiting distance between pair of protons allowing the relevability of a NOE can be assessed to about 2.4 Å (assuming comparable self-relaxation rates).

MeOD to the more viscous solvent DMSO in which the reorientational tumbling of the complex slows down.

A further issue has to be checked at this point: that the structure of the two complexes is independent of solvent composition. Such a conservation was verified on the phenyl derivative repeating the NOE experiments performed in CD_3OD: the same results were obtained in DMSO and acetonitrile. Furthermore, on changing the temperature, the absence of observable dynamic processes involving the DOTA-portion of the molecule was also demonstrated in the other solvents.

In the case of Yb−(*S*)-**2** in DMSO, upon saturating the C_1 resonance at −16.2 ppm, an NOE was revealed on the E_2 peak at 12.0 ppm. Such an effect is distinct and *negative*, since the slow-motion regime has been reached, and proves that the conformation of the complex is of *n*-form, as found for the phenyl analogue. The configuration of the complex in solution is therefore $\Lambda(\delta\delta\delta\delta)$ or $\Delta(\lambda\lambda\lambda\lambda)$; it will be demonstrated that the former is the case for an R configuration at carbon, the latter for S.

c. Coordination Dynamics. The NOE experiments in different solvents unambiguously demonstrate that the conformation of the complexes is the same, independent of the solvent, and it is square anti-prismatic, as the crystal structure had suggested. The explanation of the change in the anisotropy term D in each case must imply that there is a change in axial coordination as the solvent is varied.

Useful information can be achieved by analyzing the behavior of the NMR spectra while changing the composition of the solvent. The addition of a different solvent causes a progressive variation of the position of the peaks, and hence of the associated apparent D parameter. For example, starting from pure acetonitrile, adding less than 1% of water or DMSO is sufficient to obtain a spectrum that is very similar to that in the pure new solvent. Thus in CD_3CN/water or CD_3CN/DMSO mixtures, the magnetic anisotropy apparently continuously shifts from 3500 (starting value in CD_3CN) to 3000 (water) or 1800 (DMSO). Moreover, in the latter case the growth of a new broad peak at 2 ppm appears. It has been shown[19] that in wet CD_3CN, Yb−(*S*)-**1** is axially bound to water, which resonates as an exchange-broadened signal to higher frequency of all other resonances. The appearance of the unbound water peak at 2 ppm suggests a competition between DMSO and acetonitrile, the latter being released upon addition of the former. Unfortunately, we were not able to observe the correspondent signal for the bound (nondeuterated) DMSO, which we assume to be too broad to be detected.

It is noteworthy that this continuous change in the spectral width must be interpreted as a rapid equilibrium between two species with well-defined D values. Adding 1 μL of DMSO to a 500 μL of CD_3CN solution, one observes very broad signals for all peaks, which separate at lower temperature (−40 °C) into two sets: a minor form with larger D_m, and a major form with smaller D_M. Comparing the magnetic anisotropies at different temperature is not straightforward, since this parameter is strongly *T*-dependent. Nevertheless a reasonable scaling leads us to estimate the following values at 25 °C:

$$D_m \approx 5000$$

$$D_M \approx 3000$$

Adding larger quantities of DMSO, the lines narrow and the minor form disappears.

It seems reasonable to expect that the value of D_m corresponds to that in pure acetonitrile, which is not the case. Our interpretation is that in this solvent, containing a non-negligible amount of water, there is an equilibrium between an anhydrous and a hydrated species, which is fast and leads to the observed shifts. Indeed, once more depending on the quantity of H_2O, one obtains different spectral widths and also different line widths. At low temperature this solvent-exchange process can be slowed sufficiently so that the coordinated water may be directly observed (Figure 2).

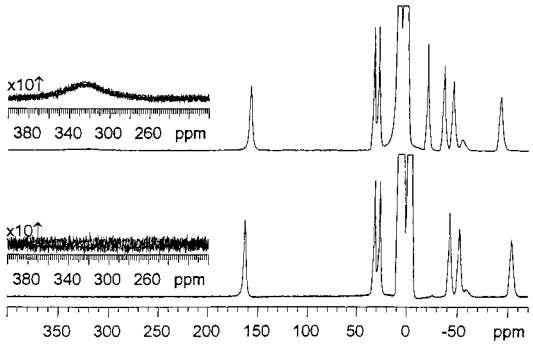

Figure 2. ^{1}H NMR spectra of Yb−(*R*)-**1** (65.3 MHz) at 233 K in CD_3OD (lower) and CD_3CN highlighting the bound water resonance at +325 ppm in CD_3CN. The small broad resonance at ∼−60 ppm is an instrumental artifact. The amide NH resonance at −20 ppm has undergone H/D exchange in CD_3OD.

In this case the spectra were acquired at −40 °C (10 mM Yb−(*R*)-**1** and 80 mM H_2O, 65.3 MHz) and the bound water resonates at +325 ppm, that is, 321 ppm to higher frequency of the free water resonance ($\Delta\nu$ = 21,000 Hz). At −35 °C the coordinated water signal broadens to such an extent that it may not be observed. In a separate study, the ^{1}H NMR spectrum of a 10 mM solution of dried Yb−(*R*)-**1** in dry CD_3CN was recorded and revealed a 4H singlet for the most shifted axial ring proton at +117.7 ppm and an exchange-broadened water resonance at +19 ppm (295 K, 200 MHz), integrating to 10 water protons. Incremental addition of water, measuring the H_2O integral to assess stoichiometry caused the water resonance to sharpen and shift to higher frequency, as before, and the position of the axial protons shifted toward a limiting value of +98 ppm. Plotting the change in shift as a function of added water concentration gave a binding isotherm which suggested that the apparent dissociation constant for water exchange in MeCN is 50 (±10) mM. These observations are compatible with the apparent water dissociation constant of 40 (±10) mM (310 K) determined independently by luminescence studies[19] as discussed in more detail below.

The total concentration of competing ligands, such as water or DMSO, affects the system through two distinct mechanisms. In the first place it perturbs the equilibrium involving the differently solvated species, each of which is characterized by different D values. Second, it affects the rate of solvent exchange between these species. At 300 MHz and in the range of temperature observed, the rates are close to the intermediate exchange regime, easily switching from fast to slow exchange.

2. NIR−CD Spectra. a. Methanol Solutions. The derivation of the distortion of the coordination polyhedron from the nature of the remote chiral centers is impossible, a priori, because of the absence of any clear relationship between the (known) chirality of the asymmetric carbons on the lateral substituents and the (unknown) chiralities of the ring and the layout of the pendant arms. The problem thus becomes a configurational assignment of the absolute stereochemistry about the metal ion. Chiroptical data can provide the desired information. For this purpose, the electronic properties connected with the unfilled *f*

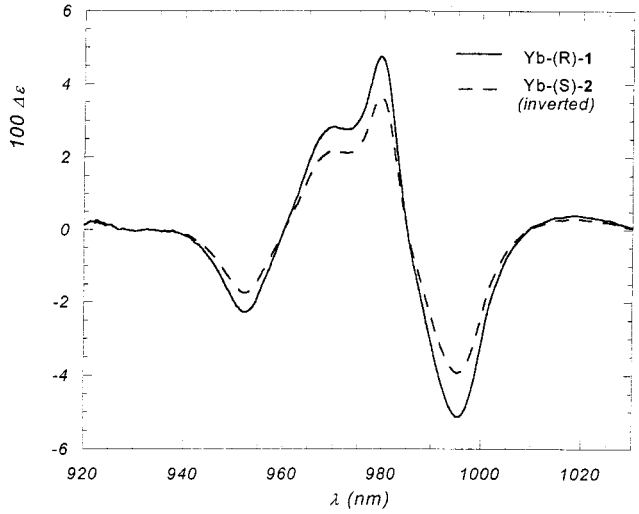

Figure 3. NIR-CD spectra of complexes Yb−(*R*)-**1** (continuous line) and Yb−(*S*)-**2** (dashed line) in MeOH solutions (c = 58.6 mM and 83.1 mM; l = 1). To make the comparison easier, the curve for Yb−(*S*)-**2** has been inverted.

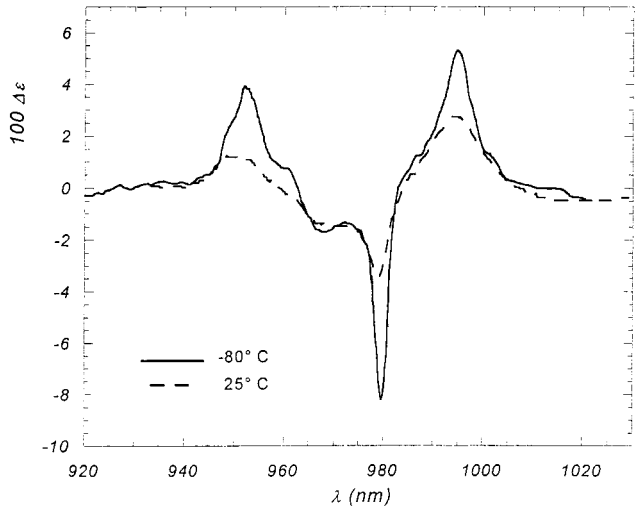

Figure 4. NIR-CD spectra of Yb−(*S*)-**2** in methanol at 25° (dashed line) and at −80 °C (continuous line) (c = 20 mM; l = 1 cm).

shell of ytterbium can be exploited and a comparison with similar compounds of definite stereochemistry can be used for an unequivocal assignment.

The near-infrared CD spectra of compounds Yb−(*R*)-**1** and Yb−(*S*)-**2** are shown in Figure 3.

The unique $f-f$ transitions of Yb^{3+} between the $^2F_{7/2}$ and $^2F_{5/2}$ states are split by a the crystal field into 4 and 3 doubly degenerates sublevels, respectively. This is globally magnetically allowed ($\Delta J = 1$) and can be classified among the most "CD sensitive" of the rare-earth family.[33] Owing to the small energy separation between the states of the lower term (of the order of 100 cm^{-1}), a temperature-dependent Boltzmann distribution of the populations of the four states of the $^2F_{7/2}$ is expected. Thus, up to 12 transitions might be observable about the center of gravity. The latter must be around 980 nm, as observed for the free ion, as it is weakly influenced by the crystal field splitting.

In the case of Yb−(*S*)-**1**, fluorescence emission spectra have been recently reported;[17] the results described herein constitute the absorption counterpart and are an important complement, being related to the ground-state chirality.

Due to the large number of superimposing hot bands and to the line width of the signals, no detailed interpretation is feasible. The spectra of the two complexes are identical as far as the overall pattern is concerned (that is the band positions and relative intensities); the only difference is in the amplitude of the signals. This seems to suggest that the electronic properties of the central cation are dependent on the first coordination sphere only, whose distortion must in turn be insensitive to the replacement of the aromatic moiety. Such a conclusion is in agreement with that found in the fluorescent emission studies.[17]

For each molecule, both in absorbance and in CD, four main peaks were easily identified at 946, 975, 982, and 995 nm, with bandwidths of 10−20 nm; a fifth weak and broad signal was recognized at around 1020 nm. The dissymmetry factors calculated for the 995 nm band g^{995}_{abs} are 0.18 for Yb−(*R*)-**1** and slightly less (0.16) for Yb−(*S*)-**2**.

b. Comparison with YbDOTMA. It is instructive to compare the aforementioned results with the NIR-CD spectrum of another C_4 symmetric ytterbium complex, (*R*)-YbDOTMA, which has been recently reported and whose structure has been determined to be of $\Lambda(\delta\delta\delta\delta)$ type.[14] In the latter case, the coordinating oxygens of the ligand are charged carboxylates. The nature of the oxygen donor determines the magnitude of the crystal field splitting, believed to have a strong contribution from atomic charges. This can be the cause of the fact that the spectra of compounds Yb−(*R*)-**1** and Yb−(*S*)-**2**, which feature neutral amide carbonyls, cover a much narrower range (940−1020 nm compared to 915−1060 nm).

Notwithstanding the difference in spectral width, the similarity between the two sets of spectra, once the narrowing effect is taken into account, is striking. Also the relative amplitudes of the individual signals are comparable, with a g factor for the component at 980 nm in YbDOTMA calculated to be 0.2.

These features are sufficient to allow a safe correlation to be drawn for the stereochemistry of the metal center. By combining the information obtained from NMR, the conformation of the two (*R*)-amide complexes can now be definitely described as $\Lambda(\delta\delta\delta\delta)$. Moreover, in solution as well, for each of these complexes, the same chirality of the substituents on the sidearms, whatever their position with respect to the ring, determines the same overall distortion of the coordination polyhedron ((*R*) → Λ; (*S*) → Δ), which in turn is translated into the same sign sequence for the main CD bands in the NIR region.

c. Variable Temperature Data. To gain further insight into the composition of the CD pattern, a low-temperature spectrum of Yb−(*S*)-**2** in methanol solution was recorded (Figure 4).

At −80 °C, the position of the signals does not change, but all the lines become narrower and, consequently, more intense. The effect is more pronounced for the band at 980 nm, which can thus probably be assigned to a transition originating from the ground crystal field sublevel of the $^2F_{7/2}$ state. Unfortunately, the narrowing of the other bands is not sufficient to allow a clear assignment of the crowded pattern, unlike for Yb-DOTMA.[14] As a consequence of the weaker crystal field, not only do many signals fall into a narrower spectral window, but the hot bands also remain significantly populated even at −80 °C.

d. Variable Solvent Data. The relationship suggested between the crystal field splitting and the CD pattern deserves further consideration, particularly in relation to the variation of the D factor revealed by the NMR.

The CD spectra of the complexes do not change appreciably on varying the solvent from (wet) acetonitrile to water or (wet) methanol, consistent with the minor changes seen by ^1H NMR. At the same time, the large variations recorded by both spectroscopies upon switching to DMSO solutions (Figure 5)

(33) Richardson, F. S. *Inorg. Chem.* **1980**, *19*, 2806−2812.

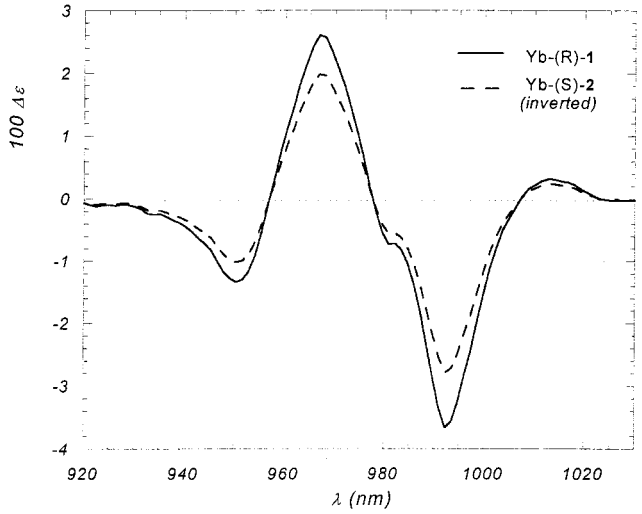

Figure 5. NIR-CD spectra of complexes Yb−(*R*)-**1** (continuous line) and Yb−(*S*)-**2** (dashed line) in DMSO solutions (c = 59 mM and 83 mM; l = 1). To make the comparison easier, the curve for Yb−(*S*)-**2** has been inverted.

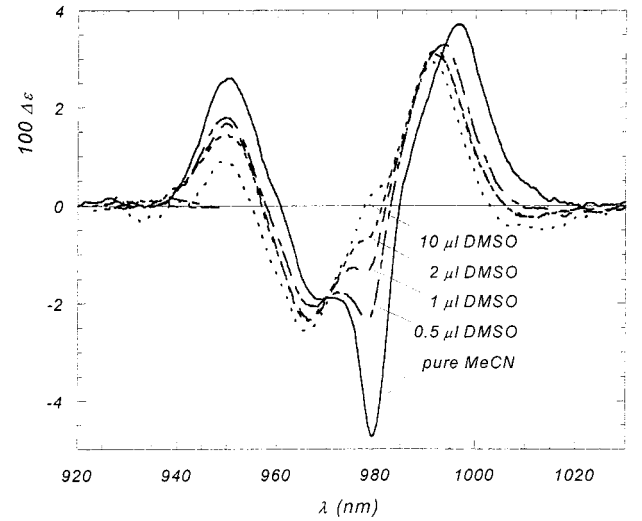

Figure 6. NIR-CD spectra during the titration of MeCN solution of Yb−(*S*)-2 with DMSO (c = 20 mM, l = 1; DMSO added up from 0.5 μL to 10 μL in a 0.5 mL solution of MeCN).

clearly demonstrate the correspondence between electronic spectra and magnetic properties of the Yb center. NOE evidence led us to discard a structural rearrangement as the origin of the change in the magnetic anisotropy constant D, which instead is attributed to a different axial coordination equilibrium in the different solvents. The same mechanism apparently plays a role in determining the energy of the electronic states observed by NIR CD.

It is noteworthy that the spectral width and the amplitude of the signals are comparable in the two solvents (methanol and DMSO) for each species, and that the relative intensities associated with complexes Yb−(*R*)-**1** and Yb−(*S*)-**2** are the same in each case. The sign sequence is indifferent to the solvent as well.

Figure 6 shows the variation of the CD profile of Yb−(*S*)-**2** in acetonitrile (10mM) following incremental addition of DMSO. After addition of 10 μL of DMSO, the spectrum became the same as that recorded in pure DMSO solution and did not change any further thereafter. Such behavior is fully compatible with the NMR data discussed above and supports the hypothesis

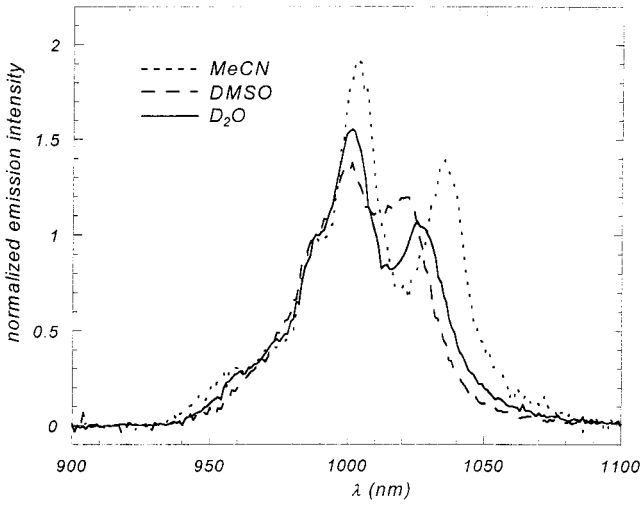

Figure 7. Emission spectra for Yb−(*R*)-**1** recorded in MeCN, D_2O and dry DMSO (310K, 1 mM complex, $\epsilon_{exc.}$ = 266 nm).

of a solvent exchange process involving the displacement of the bound H_2O or MeCN ligand by a DMSO molecule.

3. Luminescence Data. Dried samples of Yb−(*R*)-**1** and Yb−(*R*)-**2** were dissolved in anhydrous acetonitrile or D_2O (H_2O) to give 1 mM solutions. The rate of decay of the Yb luminescence was monitored at 310 K following excitation into the phenyl rings at 266 nm, using methods described previously.[24] For Yb−(*R*)-**1**, the rate of decay in H_2O was $1.4 \cdot 10^6$ s^{-1} and fell to $0.13 \cdot 10^6$ s^{-1} in D_2O; with Yb−(*R*)-**2**, the corresponding figures were $1.25 \cdot 10^6$ s^{-1} and $0.20 \cdot 10^6$ s^{-1} respectively. Given the established sensitivity of the Yb excited state to quenching by OH oscillators, these data are consistent with hydration states of 1.07 and 0.85 for Yb−(*R*)-**1** and Yb−(*R*)-**2**, after allowing for the effect of unbound (closely diffusing) OH oscillators which give rise to a quenching effect estimated to be $0.2 \cdot 10^6$ s^{-1}.[24] In dry acetonitrile the rate of decay was measured to be $0.4 \cdot 10^6$ s^{-1} for Yb−(*R*)-**1** and the same value was recorded for Yb−(*R*)-**2**. Thus, under these experimental conditions, the data in acetonitrile show that the dried sample is not bound to a water molecule. Accordingly, water was added incrementally to this solution and the rate of decay of the Yb excited state was observed to increase toward a limit of ca. $1.35 \cdot 10^6$ s^{-1}. By plotting the change in k_{obs} as a function of water concentration and assuming a 1:1 binding stoichiometry, the equilibrium constant for water association (strictly this is for exchange of MeCN by water) was estimated to be 40 M^{-1}. Thus K_d is 25 mM for dissociation of water from Yb−(*R*)-**1**·(H_2O), so that the water is not associated significantly at low complex concentrations in dried MeCN. A similar value for K_d of 42 mM has been measured for Eu−(*S*)-**1** in MeCN [19] by observing changes in the decay of the Eu excited state.

These changes in axial solvation were also characterized by changes in the form of the emission spectrum of each complex. The emission spectra for Yb−(*R*)-**2** (10 μM) were measured in dry MeCN, D_2O, and dry DMSO (Figure 7), following excitation of the naphthyl chromophore at 305 nm. Very similar spectra were recorded for Yb−(*R*)-**1**, under identical conditions, following excitation at 255 nm. With the much lower concentrations used to obtain these spectra, there is little chance of adventitious water preferentially associating, and the solvents used were dried to less than 10 ppm water. The emission bands at 980 and 1000 nm varied only slightly in relative intensity. However, the longest wavelength emission band shifted from 1020 nm in DMSO to 1025 in D_2O and 1035 nm in MeCN. The observed solvent dependence is consistent with the behavior

revealed by the near-IR CD studies, and supports the conclusion that the nature of the axial donor is very important in determining the crystal field splitting.

Conclusions

From the data collected, it is clear that a strong correspondence can be observed between magnetic and optical parameters used in describing the behavior of lanthanide ions in solution. Although such a correspondence cannot be fully rationalized, it provides a confirmation of the hypothesis of Bleaney[28] which has almost never been tested by a thorough experimental study.[34]

Furthermore, analyzing the ^{1}H NMR spectra of the whole family of DOTA-derivatives, it is evident that there are different processes contributing to the values of the magnetic anisotropy D: structural rearrangements and hydration-dehydration processes (or coordination number). The observed D factor can be considered as the sum of two terms:

$$D = D_{ax} + D_{lig}$$

in which D_{ax} is a function of the nature of the axial ninth ligand and D_{lig} is the contribution brought about by the coordination of the macrocyclic ligand. The D_{lig} term is also sensitive to the shape of the coordination polyhedron, assuming different values in the case of distorted anti-prismatic and regular anti-prismatic coordination geometries.

The simultaneous occurrence of structural rearrangement and hydration/dehydration often reported in the literature has somewhat obscured the latter process in favor of the former. Thus, the variation in the observed D has been related to a conformational change. Moreover, the similarity between complexes based on N-alkylated tetraazacyclododecanes (cyclen) has perhaps been over-emphasized, by extrapolating data involving complexes with different donor atoms. The present work demonstrates that the parameter D for Yb(III) is very sensitive to the nature of axial ligand and that no simple structural information can be directly extracted from it.

Although the present study is limited to Yb(III) complexes, the conclusions go beyond the behavior of this ion: Ytterbium among the lanthanides can be considered an extreme system, since the induced shifts are almost completely dipolar in nature; the results obtained can thus be generalized to all the paramagnetic lanthanides for which the pseudocontact term is not negligible with respect to the contact contribution to the chemical shift, this means all elements besides Pm^{3+}, Sm^{3+}, Eu^{3+}, and Gd^{3+}.

We have shown that stereochemical analysis on this class of molecules requires care and the complementary use of different techniques is strongly advised. ^{1}H NMR shift data provides a powerful tool for structural refinement but yields information on isomeric forms which cannot be simply discriminated. Only by NOE measurements can one assign which is the more stable structure in solution.

Despite the detailed information obtained by these methods, it may seem surprising that the local stereochemistry around the metal ion is still not defined. Indeed, the fact that the stereogenic center is remote from the inner sphere, justifies the absence of experimental configurational correlation.

In solution, NIR-CD spectroscopy provides this information, by relating the spectrum to that of YbDOTMA, which has been fully assigned and confirms the absolute configuration determined by the earlier X-ray crystallographic study.

Finally, examination of luminescence data (i.e., the rate of decay of the Yb emission and the form of the emission spectrum itself) completes the picture about the nature of the axial donor providing a link to the chiroptical results and to the solution NMR interpretation.

Even though much work has to be done for the full interpretation of the intimate relationship between electronic and magnetic properties of ytterbium in these and similar compounds, the concerted application of NMR, luminescence, and NIR-CD spectroscopy can allow a deeper understanding of the coordination properties of these attractive complexes.

Acknowledgment. We thank CNR and EPRSC for support and Dr. Andrew Beeby (University of Durham) for assistance with the Yb emission work.

JA0012568

(34) Babushkina, T. A.; Zolin, V. F.; Koreneva, L. G. *J. Magn. Reson.* **1983**, *52*, 169−181.